



DIGITAL ACCESS TO
SCHOLARSHIP AT HARVARD
DASH.HARVARD.EDU



HARVARD LIBRARY
Office for Scholarly Communication

Dynamics of BAF- Polycomb Complex Opposition on Heterochromatin in Normal and Oncogenic States

The Harvard community has made this
article openly available. [Please share](#) how
this access benefits you. Your story matters

Citation	Kadoch, Cigall, Robert T. Williams, Joseph P. Calarco, Erik L. Miller, Christopher M. Weber, Simon G. Braun, John L. Pulice, Emma J. Chory, and Gerald R. Crabtree. 2016. "Dynamics of BAF- Polycomb Complex Opposition on Heterochromatin in Normal and Oncogenic States." <i>Nature genetics</i> 49 (2): 213-222. doi:10.1038/ng.3734. http://dx.doi.org/10.1038/ng.3734 .
Published Version	doi:10.1038/ng.3734
Citable link	http://nrs.harvard.edu/urn-3:HUL.InstRepos:33490902
Terms of Use	This article was downloaded from Harvard University's DASH repository, and is made available under the terms and conditions applicable to Other Posted Material, as set forth at http://nrs.harvard.edu/urn-3:HUL.InstRepos:dash.current.terms-of-use#LAA



Published in final edited form as:

Nat Genet. 2017 February ; 49(2): 213–222. doi:10.1038/ng.3734.

Dynamics of BAF- Polycomb Complex Opposition on Heterochromatin in Normal and Oncogenic States

Cigall Kadoch^{1,2,*}, Robert T. Williams¹, Joseph P. Calarco³, Erik L. Miller³, Christopher M. Weber³, Simon G. Braun³, John L. Pulice^{1,2}, Emma J. Chory³, and Gerald R. Crabtree^{3,*}

¹Department of Pediatric Oncology, Dana-Farber Cancer Institute and Harvard Medical School, Boston, MA, USA.

²Broad Institute of MIT and Harvard, Cambridge, MA, USA.

³Howard Hughes Medical Institute and Departments of Pathology and Developmental Biology, Stanford University School of Medicine, Stanford, CA, USA.

Abstract

The opposition between polycomb repressive complexes (PRC) and BAF (mSWI/SNF) complexes plays critical roles in development and disease. Mutations in the genes encoding BAF subunits contribute to over 20% of human malignancy, yet the underlying mechanisms remain unclear owing largely to a lack of assays to assess BAF function in vivo. To address this, we have developed a widely applicable recruitment assay system and find that BAF opposes PRC by rapid, ATP-dependent eviction, leading to the formation of accessible chromatin. Reversing this process results in reassembly of facultative heterochromatin. Surprisingly, BAF-mediated PRC eviction occurs in the absence of PolII occupancy, transcription, and replication. Further, we find that tumor suppressor and oncogenic BAF complex mutations result in differential effects on PRC eviction. These studies define a mechanistic sequence underlying the resolution and formation of facultative heterochromatin and demonstrate that BAF opposes polycomb complexes on a minute-by-minute basis to provide epigenetic plasticity.

INTRODUCTION

The portion of the genome available to regulatory mechanisms appears to reflect a balance between chromatin processes that favor accessibility and those that oppose it. This balance was first recognized in *Drosophila*, in which the trithorax group of genes was shown to favor activation of developmental genes, while polycomb genes were found to oppose activation¹. The trithorax genes encode enzymes that produce the activating histone modification

Users may view, print, copy, and download text and data-mine the content in such documents, for the purposes of academic research, subject always to the full Conditions of use:http://www.nature.com/authors/editorial_policies/license.html#terms

***Corresponding Authors:** Gerald R. Crabtree, Howard Hughes Medical Institute, Stanford University School of Medicine, 279 Campus Drive; Rm B211, Beckman Center, Stanford, CA 94305-5323, Phone: 650-723-8391, crabtree@stanford.edu. Cigall Kadoch, Dept. of Pediatric Oncology, Dana-Farber Cancer Institute, Harvard Medical School, 450 Brookline Avenue; Dana D620, Boston, MA 02215, Phone: 617-632-3789, Cigall_Kadoch@dfci.harvard.edu.

Author Contributions

C.K. and G.R.C. conceived of the study and wrote the paper. C.K., R.T.W., J.P.C., C.M.W., E.L.M., S.G.B. and E.J.C. planned and performed the experiments. J.L.P. performed data analysis and statistics.

H3K4me3 or the BAP (Brahma Associated Protein) ATP-dependent chromatin remodeling complex²⁻⁴. Genetically, trithorax proteins act in opposition to the polycomb genes, which encode the subunits of the Polycomb repressive complex 1 (PRC1) and 2 (PRC2). These complexes direct H2A ubiquitination and H3K27me3 modification, respectively, favoring inaccessible chromatin⁵. The presence of PRC1 and PRC2 is a mark of 'facultative heterochromatin', which is distinguished from constitutive heterochromatin at centromeres and other regions of the genome.

Genomic studies have revealed that the genes involved in this opposition are frequently mutated in human cancer. Subunits of the mammalian mSWI/SNF or BAF (for Brg/Brm associated factor) complexes are mutated in over 20% of all human cancers^{6,7} and a large number of human neurologic diseases⁸⁻¹¹. These complexes promote accessibility at least in part by opposing the actions of polycomb complexes^{12,13}. The MLL genes are catalytic subunits of the Compass complex and place the activation-associated H3K4me3 modification¹⁴, and are mutated in a large number of somatic cancers⁴. The repressive PRC2 subunit EZH2 is mutated or silenced in a number of leukemias and lymphomas^{15,16,17}.

In mammals, BAF complexes are combinatorially assembled into 15-subunit assemblies encoded by 29 genes, giving rise to highly polymorphic complexes that can be exquisitely cell type-specific, such as the nBAF complex found only in post mitotic neurons^{18,19}. The BAF subunit mutations in human cancer have a striking pattern of tissue specificity. For example, nearly 100% of cases of human synovial sarcoma are produced by the SS18-SSX (t(X;18) translocation, however the SS18 BAF subunit is rarely mutated in other cancers. Malignant rhabdoid tumors (MRTs) are uniformly produced by deletions or loss-of-function mutations in BAF47 (hSNF5), but this subunit is less frequently involved in other human cancers²⁰. Present data indicate that the mechanisms of oncogenesis appear to relate to the ability of BAF complexes to oppose polycomb-mediated repression. In human MRTs, loss of BAF47 leads to polycomb-mediated repression of genes that suppress proliferation, such as *INK4A*²¹ and reexpression of BAF47 leads to removal of polycomb and loss of DNA methylation by an unknown mechanism(s)²². While informative, long time courses of reexpression in these earlier experiments prevented direct mechanistic analysis and the removal of polycomb could have been due to differentiation, replication or other cell biologic actions. Nevertheless correlative studies suggested that BAF might evict polycomb at this locus. Conversely, in synovial sarcoma, the SS18-SSX oncogenic fusion protein, which is the product of the oncogenic allele dominantly assembles into BAF complexes, targeting them to silenced polycomb target genes, where it appears to remove polycomb²³. However, it is not known if the BAF-Polycomb balance is achieved directly or indirectly, nor is there any knowledge of causal sequence of biochemical events that provide this critical balance.

The mechanism underlying BAF-Polycomb opposition has been difficult to study. This is because present in vitro approaches using nucleosomal templates are unable to mimic the effects of tissue-specific histone modifications, long-range interactions, topological features, and post-translational modifications of the proteins involved. To elucidate the mechanism, we developed a method to rapidly and reversibly recruit a chromatin regulator of interest to one allele of an endogenous gene and then measure and model the sequence of biochemical

events at this locus. We find that BAF complex recruitment evicts both PRC1 and PRC2 within 5 minutes followed by the development of accessibility. The order of deletion and reappearance predicts that PRC1 activity precedes PRC2 activity. These studies reveal that, in contrast to expectations, BAF complexes opposes both PRC1 and PRC2 on a minute-by-minute basis without need for replication, PolIII occupancy, or transcription.

RESULTS

Development of an assay system to study the mechanism of BAF-Polycomb opposition

To study the opposition between BAF and polycomb at repressed facultative heterochromatin, we modified the endogenous *Oct4* (*Pou5f1*). The *Oct4* locus in MEFs is repressed by polycomb complexes^{24,25} and H3K9me3²⁶ and lacks BAF complex occupancy; by contrast, in pluripotent cells, the locus lacks Polycomb and instead has robust Brg1 (Smarca4) binding over the proximal enhancer, which is essential for Oct regulation^{12,27–29} (Supplementary Fig. 1a). To analyze the resolution of heterochromatin by BAF we developed the CIAO mouse (Chromatin Assay at and Indicator at Oct4) by modifying one *Oct4* allele with two different arrays of transcription factor bindings sites upstream of the transcription initiation site³⁰ (Fig. 1a, Supplementary Fig. 1b). In addition, GFP was inserted into the Oct4 allele allowing visualization of active cells, but inactivating one allele. The allele containing the insertions is regulated similarly, both qualitatively and quantitatively, to the unmodified allele and that histone modification are indistinguishable (Supplementary Fig. 1c, Fig. 1b). These observations indicate that local and long-range topologic features are not disturbed on the modified allele and that the insertion does not modify the pattern of histone modifications. The Oct4 allele containing the insertions is active in pluripotent cells and germ cells derived from the CIAO mouse, but intensely repressed in fibroblasts by polycomb group marks such as H3K27me3 as well as H3K9me3 (Fig. 1c). The *Oct4* locus undergoes repression upon ES differentiation³⁰, and in fibroblasts, the gene can only be activated after prolonged exposure to the core pluripotency factors³¹.

This system provides a broadly applicable model for developmental chromatin regulation allowing the temporally precise addition of one specific factor within a context of normal chromatin. While signaling pathways such as the LIF-STAT3 pathway also induce chromatin changes, LIF responses are too diverse, involve too many chromatin regulators and too asynchronous to allow mechanistic interpretation^{12,32}. We used the CIP (Chemical Inducer of Proximity), rapamycin, to induce proximity of proteins at the modified *Oct4* allele by virtue of its ability to bind one protein tag (Frb) on one side and another tag (FKBP) on the other side of the molecule (Fig. 1a). Because rapamycin binding is diffusion-limited and the off rate is on the order of seconds, this approach does not produce a rigid topology, but rather a cloud of complexes^{33,34}. This is in contrast to direct fusions, which produce rigid conformations that can sterically restrict the activity of the recruited proteins. Thus, the recruited BAF complex is free to assume its normal mode of binding to the Oct4 locus. To induce proximity of the BAF complex, we chose to fuse the SS18 subunit to Frb because SS18 remains stably associated with the BAF complex to 5M urea and is also a dedicated subunit^{23,35} (Fig. 1d). We confirmed proper complex assembly of the Frb-V5-tagged SS18 subunit (Supplemental Fig. 1d), as well as Frb-V5-tagged BAF47 and BAF57 subunits

(Supplemental Fig. 1e). We fused FKBP to the DNA binding domain of the ZFHD1 zinc finger, to bind the ZFHD1 sites inserted ~250 bp upstream of the *Oct4* promoter within a large repressed, H2Aub1, H3K27me3- and H3K9me3- decorated domain in fibroblasts (Supplemental Fig. 1b). We evaluated the feasibility and robustness of this system using three BAF complex subunit fusions and determined that within 24 hours, BAF complex recruitment was induced 40–60 fold over baseline levels and that the SS18 subunit-based recruitment was optimal (Fig. 1e, Supplemental Fig. 1f). This strategy is a chemical-genetic gain-of-function approach that only requires a few dozen binding events to induce recruitment to the single allele, thereby allowing the endogenous mTor (FRB) and FKBP12 molecules to perform their normal functions^{30,33}.

Remarkably, addition of 3.0 nM rapamycin recruited the entire 2 MDa BAF complex to the *Oct4* locus with a lag time of only 2 minutes ($t = 2.2 < t < 4.8$ min, $CI = 95\%$) and at levels similar to BAF peaks over the genome of ES cells (Supplemental Fig. 1g). To be certain that the complexes were fully assembled, we performed ChIP experiments using antibodies to V5 (to capture the Frb-V5-SS18 bearing complexes), as well as Brg1 and Baf155 and found that each was effectively recruited within 2–5 minutes (Fig. 1f, Supplemental Fig 1h, left and right). Importantly, the levels and extent of BAF binding by 3 nM rapamycin were similar to BAF peaks over the genome²⁷. BAF complexes occupied a region of approximately 1200 bp, consistent with binding of a single 2MD complex⁶ (Fig. 1g). Based on published studies³⁶, we calculate the fractional occupancy at about 20% and the dwell time <83 seconds indicating that the recruited complexes are maintained at this location in part by direct interactions with facultative heterochromatin. Thus, using this CIP system, BAF complexes can be recruited, at normal levels and dynamics within minutes.

Recruitment of BAF complexes results in rapid eviction of PRC complexes

Mutations of the *Drosophila* BAP (dSWI/SNF) ATPase, *Brm*, entirely suppresses the effects of PRC1 mutations on body plan morphogenesis, attesting to their functional dedication^{13,37,38}. Importantly, BAF-PcG opposition has become increasingly recognized as an oncogenic mechanism in several human cancers^{21,23,39}. Thus we first measured the effect of BAF recruitment on PRC eviction (Fig. 2a). We find that recruitment of BAF leads to the removal of both the PRC2 complex (Ezh2) and the H3K27me3 mark within minutes (Fig. 2b, Supplementary Fig. 2a). We also tested the alternative possibility that BAF recruitment removes PRC2 complexes with subsequent loss of H3K27me3 by comparing the time-course of their removal after recruitment of the BAF complex. Unexpectedly, we found a full 10-minute lag between the removal of PRC2 (Ezh2) and the initial reduction of H3K27me3 ($t(lag) = 9.22 < t < 11.41$ min) (Fig. 2b). This lag-time is unlikely to reflect differences in antibody detection, since the modification is more abundant than the enzyme.

PRC2 works in synergy with PRC1 to repress genes² and both PRC complexes and their associated histone marks and complexes are present at the repressed *Oct4* gene of fibroblasts. In flies, PRC1 (the pc1 or CBX6 subunit) mutants are repressed effectively by mutations in the ATPase *Brm*¹³. Remarkably, PRC1 complexes disappeared from the repressed *Oct4* locus with even faster kinetics compared to PRC2, as assayed by ChIP using an antibody to Ring1b (Fig. 2c). Eviction of PRC1 was paralleled by dissolution of the

H2Aub1 repressive mark (Fig. 2c). Decreased occupancy of the H2AK119ub mark preceded the decreased occupancy of the H3K27me3 mark (Fig. 2d, right).

These observations raised the question as to whether BAF recruitment-mediated PRC displacement was a result of increased rate of nucleosome or histone exchange, as previous studies have shown that BAF complexes can exchange nucleosomes in vitro; although this possibility has not been tested in vivo^{40,41}. We found that within the first hour there was no detectable change in the levels of H3K9me3, the other prominent repressive mark at this locus, or total H3, or H2A.Z, suggesting that the removal of H3K27me3 resulting from BAF complex recruitment does not reflect a non-specific enhancement of nucleosomal turnover (Fig. 2d left, Supplementary Fig. 2b).

Because we unexpectedly could not detect H3 depletion after BAF complex recruitment, we developed another murine model system by double knock-in of the DNA-binding sites and GFP reporter, which we call CiAA (Chromatin indicator and Assay at *Ascl1*). Here we used the *Ascl1* locus which encodes the neuronal pioneer factor *Ascl1*, which has both H3K27me3 and H3K4me3 over its regulatory regions and has a CpG island, often seen at PRC- marked sites^{42,38}. *Ascl1* promoter is occupied by polymerase and the promoter accessible (ENCODE data). Hence, *Ascl1* in ES cells is quite different than Oct4 in fibroblasts and allowed us to test the robustness of our findings. Similar to Oct4 in MEFs, we found that BAF recruitment led to eviction of PRC1 and 2 within 2 minutes (Stanton et al. (NG-LE43713R, accepted). Addition of rapamycin resulted in robust recruitment of (Supplemental Fig. 2c). In contrast to the highly repressed Oct4 locus in MEFs, we were able to detect H3 turnover using CATCH-IT analysis⁴³ and also depletion of H3 by CHIP (Supplemental Fig. 2c). Thus, it appears that polycomb eviction occurs without detectable H3 or H3K9me3 depletion at the facultative heterochromatin of the Oct4 locus of MEFs, but H3 exchange is clearly detectable in ES cells at the accessible *Ascl1* locus upon BAF recruitment.

We predicted that if Polycomb contributed significantly to repression of the Oct4 locus we would find enhanced accessibility over the recruitment sites corresponding to either the removal of the H3K27me3 mark or of polycomb complexes. We assayed accessibility using a modified ATAC-seq assay which measures the ability of the Tn5 transposase to invade open, but not closed chromatin (Supplementary Fig. 2d,e)⁴⁴. Remarkably, the development of accessibility as reflected by lag-times quickly followed the near maximum removal of H3K27me3 and H2Aub1 (Fig. 2e, Fig. 2b,c). Accessibility was restricted to the recruitment region of the locus and was not significantly altered at more distant regions (Supplementary Fig. 2e).

Our studies predict that BAF and PRC should colocalize over the genome. Indeed, we find that 67% of BAF sites are co-occupied by PRC1 genome-wide, strongly suggesting that these two complexes somehow cooperate (Supplementary Fig. 2f). This level of co-occupancy is higher than PRC2 with PRC1, which are known to function synergistically^{5,38}. In other studies, we have found that BAF directly binds PRC1, but not PRC2, and releases it in an ATP-dependent mechanism (Stanton et al, accepted (NG-LE43713R)).

We were concerned that steric interference by recruitment of a large complex, several fold larger than PRC1 and 12-fold larger than a nucleosome could account for polycomb eviction. Thus, we recruited the LSH (HELLS) ATP-dependent chromatin remodeler. While addition of rapamycin effectively recruited these complexes to the *Oct4* locus, we did not detect removal of PRC1 or the H2AK119ub1 repressive mark placed by this complex (Fig. 2f), indicating that PRC eviction is a specific property of BAF complexes.

Finally, Oct4 gene expression (as assayed by GFP-positive cells and mRNA levels) was not induced (Supplementary Fig. 2g), likely due to the substantial, unaltered repression by H3K9me3 (Fig. 2d), DNA methylation and lack of recruitment of RNA Pol II (Supplementary Fig. 2h). Recent studies have demonstrated that loss of PRC2 repression only activates bivalent genes with the H3K4me3 mark⁴⁵, explaining the absence of gene activation upon polycomb eviction. Thus our system allows one to deconvolute the effects of these influences on accessibility in the absence of other variables.

Repressed heterochromatin is reestablished following BAF removal

Genes active in early development such as Oct4 are often repressed by polycomb during the course of differentiation. To understand the underlying mechanisms, we studied the reassembly of polycomb-repressed heterochromatin. This was achieved using FK1012³⁴, a dimeric competitive inhibitor of rapamycin which binds only to the FKBP side and rapidly competes away rapamycin (Fig. 3a, Supplementary Fig. 3a). In comparing the kinetics of rapamycin washout (via media change) versus addition of FK1012, we determined that FK1012 resulted in more rapid, robust decreases in BAF complex tethering to the Oct4 locus (Fig. 3b), enabling us to determine if inaccessible heterochromatin could be reformed. We found that addition of FK1012 lead to the removal of BAF complexes within $t=15' < t < 30'$ minutes (Fig. 3b), as assessed by anti-V5 ChIP, and the reappearance of PRC2 (Ezh2) and H3K27me3 by $t=0.5 < t < 2.5$ hours (Fig. 3c). We found that PRC2 (Ezh2) and PRC1 (Ring1b) began to reappear within ~2 hours post-addition of FK1012 and that this was paralleled by the reappearance of H3K27me3 and H2Aub1. (Fig. 3c,d). The open, DNA-accessible state produced by BAF complex dissociation was not stable, as suggested by in vitro studies on nucleosomal templates⁴⁶, but rather, inaccessible chromatin began to reform within 2.5–5 hours after removal of the BAF complex (Fig. 3e and Supplementary Fig. 3b–e). These washout experiments mimic the developmental transition that occurs over many genes that are active in early development and later become repressed by polycomb and facultative heterochromatin. Thus, our system allows one to make kinetic determinations in vivo of both dissolution and establishment of facultative heterochromatin.

Eviction of polycomb repressive complexes and associated histone marks is dependent on the ATP-ase activity of Brg1

The ATPase activity of BAF complexes provided by the Brg1 or Brm subunits is necessary for the function of BAF complexes in a variety of assays and the ATPase domains are frequently mutated in cancer and neurologic diseases^{39,47}. Hence, we asked if the ATPase activity of Brg1 were necessary for PRC1 and PRC2 eviction. Thus, we directly recruited Brg1 by fusing the Frb tag on the C-terminus of the protein. This strategy did not give as robust recruitment of BAF as did the fusion on SS18. However, we did find that the Brg1

fusion gave about a 4- to 8-fold increase in occupancy of Baf155 at the recruitment site, as compared to SS18 fusion (40- to 60-fold). To test the role of the ATPase activity of Brg1, we used a mutation (K-to-R; K785R) with reduced ATPase activity⁴⁸ found in a number of cancers and neurologic diseases⁴⁷. Recruitment of this mutant Brg1 protein to the Oct4 locus of MEF (Fig. 4a,b) led to less PRC1 and PRC2 eviction than found with wild-type Brg1 (Fig. 4c,d). Thus, the ATPase activity of Brg1 is required for this novel activity. This result, along with the LSH recruitment studies (Fig. 2f) rules out the possibility that non-specific steric occlusion contributes to PRC eviction. The experiments above indicate that BAF complexes are capable of driving a transition between inaccessible higher order chromatin structure toward accessibility, and that this is due to the direct eviction of both PRC2 and PRC1 complexes.

Recruitment of cancer-specific BAF complexes to repressed heterochromatin

BAF complexes can behave as either oncogenes or tumor suppressors. Unfortunately, it has not been possible to directly assay the effects of these mutations using in vitro assays. Hence, we asked if we would be able to discern the mechanism of these oncogenic mutations using the CIAO assay. To this end, we recruited BAF complexes with highly specific, driving subunit mutations, which define specific cancer subtypes to polycomb-repressed chromatin. To study the consequences of recruitment of BAF complexes lacking the BAF47 (hSNF5) tumor suppressor subunit, the hallmark feature of pediatric malignant rhabdoid tumors (MRTs), we performed shRNA-mediated KD of BAF47 (KD efficiency >80%). We then recruited BAF complexes using BAF57 as the Frb-V5 tagged subunit in this case as BAF47 KD results in reduced SS18 binding into BAF complexes (unpublished results) (Fig. 5a, Fig. 1e, Supplementary Fig. 1d). Frb-V5-BAF57 tagged complexes, both wild-type and complexes lacking BAF47 displayed comparable recruitment levels to the Oct4 locus (Fig. 5b–c). Intriguingly however, BAF47-lacking complexes exhibited significantly decreased ability to displace Ezh2 (PRC2 complexes), Ring1b (PRC1 complexes) and the H3K27me3 mark at the Zinc-finger binding domain, as compared to wild-type complexes (Fig. 5d–f). This demonstrates that BAF47 loss in these tumors leads to an inability to oppose polycomb, mechanistically explaining the tumor suppressive functions previously observed at the Ink4A locus and others²¹ and justifying the therapeutic use of PRC inhibitors.

BAF complexes can also be oncogenes that both initiate and drive cancer as is the case with the SS18-SSX translocation, which is found in nearly 100% of synovial sarcomas and in nearly 100% of the cells. Hence we determined if BAF complexes with the SS18-SSX fusion could oppose polycomb. To perform these studies, we developed Frb-V5-SS18-SSX fusions to be directly compared with our measurements using Frb-V5-SS18 (wild-type) (Fig. 6a). Using anti-Brg1 immunoprecipitation, we demonstrated that these complexes bear the expected features of BAF complexes containing the SS18-SSX fusion as demonstrated previously²³; namely, reduced protein assembly of BAF47 as well as wild-type SS18 (Fig. 6b). Notably, as compared to WT SS18 containing BAF complexes, SS18-SSX BAF complexes displayed a dramatically extended domain of BAF occupancy, spreading 2620 ± 456 bp (CI=95%) into the Oct4 gene body as compared to WT SS18 (920 ± 305 bp (CI=95%)), likely reflecting gained multimerization or processivity of complexes (Fig. 6c).

While BAF complex recruitment at the zinc-finger recruitment site (+0bp) was comparable for the WT SS18 and SS18-SSX fusion over a 60-minute time course (Supplementary Fig. 4a), BAF complex occupancy at downstream sites >1000bp into the exon was achieved only by SS18-SSX oncogenic BAF complexes (Fig. 6c, Supplementary Fig. 4e). Importantly, SS18-SSX oncogenic BAF complexes robustly displaced both PRC2 and PRC1 complexes (Fig. 6d,e, Supplementary Fig. 4b–c,f–g), as well as the H3K27me3 repressive mark (Fig. 6f, Supplementary Fig. 4d,h) at +1034 bp and +2287 bp sites from the ZFHD1 recruitment site, while WT SS18 complexes were unable to achieve these effects outside of the ZFHD1±500bp region of the recruitment site. These kinetic results explain the robust removal of PRC2 and H3K27me3 over the entire *SOX2* gene in synovial sarcoma.

DISCUSSION

Our studies indicate that the mechanism by which BAF complexes oppose polycomb complexes is at least in part achieved through rapid eviction of PRC1 and PRC2 (Fig. 7). The ATPase activity of Brg1 is required for eviction, suggesting the specificity of the process and pointing toward possible mechanisms for ATPase-dead mutations in human cancers. The fact that eviction occurs within 2–5 minutes indicates that neither cell replication nor transcription is necessary for polycomb removal. This illustrates the power of the CIAO system, which enables precise temporal control over the kinetics of BAF-polycomb opposition. Because we could not detect the expected enhanced rates of nucleosome turnover for either H3K9me3 or H3, we speculate that the loss of H3K27me3 reflects the natural rates of decay due to histone demethylases and basal rates of nucleosome removal⁴³. Indeed, BAF has been reported to bind to H3K27 demethylases⁴⁹ suggesting that it might recruit these enzymes to its sites of action. Accessibility rapidly follows the loss of H3K27me3 and H2Aub1, as expected from previous studies. In our CIAO system, we essentially convert the chromatin landscape of the Oct4 gene in MEFs to be more like that in ES cells, in which the gene is active and covered by a large domain of BAF. By removing the CIP by competition (FK1012), we revert the locus to one with inaccessible chromatin consistent with a continuous opposition between the two complexes rather than a stable expression state based on nucleosome structure.

The mechanism of action that we describe in which BAF prepares a polycomb repressed locus for binding of transcription factors (Fig. 7) provides an explanation for the apparent instructive functions of specific BAF complexes. For example, switching the subunit composition to the neural specific nBAF complex in human fibroblasts converts them to a basal neuronal state that can be biased with specific transcription factors to produce types of neurons that have never been produced in culture from either ES cells or fibroblasts^{50–52}. Instructive roles have also been reported in IPS conversion⁵³, the heart field⁵⁴, the wiring of the drosophila olfactory system⁵⁵ and induction of specific types of neurons in *C.elegans*⁵⁶. The model (Fig. 7) does not reduce the need for sequence-specific or lineage-specific transcription factors, but rather suggests that BAF and its tissue-specific assemblies act to open the range of possible binding sites for such factors and may possibly also aid in the positioning of nucleosomes to allow transcription factor binding.

The SS18-SSX fusion protein, which both initiates and drives synovial sarcoma is an example of an instructive oncogenic function of an altered BAF complex²³. Addition of only 78 aa of SSX on to the C-terminus of the SS18 subunit leads to preferential assembly of the fusion protein into an oncogenic BAF complex that then targets the inactive Sox2 locus, removing polycomb and activating the expression of the Sox2 gene, which then drives proliferation. This sequence of events largely precludes a mechanism in which a transcription factor recruits BAF, because the Sox2 locus is inactive in the cell type that gives rise to malignancy and the oncogenic BAF complex can activate the Sox2 gene in fibroblasts, in which the Sox2 locus is inactive and likely not occupied by transcription factors (Fig. 7g). Our direct in vivo recruitment studies indicate that the role of the SS18-SSX fusion is to produce a complex that propagates along the chromosome to occupy a larger region than is normally occupied by BAF over the Sox2 gene in cells in which it is inactive. We find this larger region of occupancy in both BAF ChIP-seq studies in the malignant synovial sarcoma cells that bear the translocation²³ and also when we recruit the complex to the silent Oct4 locus of MEFs. The propagation of the complex leads to a larger domain of Polycomb removal and hence a greater chance that a transcription factor present in fibroblasts will bind to the now accessible chromatin prepared by the oncogenic BAF complex. This scenario nicely illustrates how these complexes can assume an instructive function (in this case uncontrolled proliferation) by allowing transcription factors present in fibroblasts to activate a gene normally only active in pluripotent cells and neural progenitors. In the same way the nBAF complex might prepare neural specific genes for activation during reprogramming of fibroblasts to neurons^{50,51}. Our studies also indicate that the loss of the BAF47 (hSNF5) tumor suppressor subunit, in malignant rhabdoid tumors, leads to substantially diminished eviction (Fig. 7f). This mechanism nicely predicts the observations in malignant cells suggesting that loci that repress proliferation, such as *Ink4a*, become intensely repressed by a domain of H3K27me3 that builds over this gene leading to a failure to halt cell division²¹. Thus, our studies provide an explanation for both the tumor suppressor (BAF47 deletion in MRT) and oncogenic (SS18-SSX fusion in synovial sarcoma) functions of BAF complexes.

Recent exome sequencing studies have revealed striking frequencies of mutations in both BAF and polycomb subunits in human cancers^{39,57}. Where studied, mutations in subunits of BAF complexes lead to altered polycomb domains over the genome that have essential functions in either oncogenesis or pluripotency^{12,21,23}. However, we and others were faced with an inability to discern whether polycomb removal was direct or indirect, or whether replication or transcription were necessary for polycomb removal as commonly assumed. Our studies indicate that this widespread opposition is being constantly and directly waged and that its plasticity lends itself well to both developmental signaling and the balance between normal proliferation and tumor formation.

MATERIALS AND METHODS

Cells and Construct Design

CiA mouse embryonic fibroblasts (MEFs) containing a modified Oct4 promoter (with 12X ZFHD1 and 6X GAL4 sites upstream of the promoter) were generated, cultured and

maintained as previously described³⁰. Briefly, lentiviral delivery constructs bearing an EF1-alpha promoter and either puromycin or blasticidin resistance were generated to contain the constructs described here (Supplemental Fig. 1b). To generate recruitable forms of BAF complexes, genes encoding individual BAF complex subunits (SS18, BRG1, BAF47, BAF57) were fused in frame to sequences encoding Frb-V5. We generated the following constructs: Frb-V5-huSS18, Frb-V5-huSS18-SSX1, Frb-V5-huBAF57, and Frb-V5-huBAF47, huBRG1-Frb-V5, huBRG1(K785R)-Frb-V5, and a control Frb-V5-STOP to be paired with co-infected ZFHD1-FKBP.

Recruitment Assays

Briefly, adherent CiA MEF cells were treated with 3nM (final concentration) rapamycin (sirolimus; Selleckchem #S1039) (ON experiments) or 3nM rapamycin followed by 30nM FK1012 (OFF/washout experiments) for prescribed times, as indicated (2.5 minutes- 24 hours). For acute time points, cells were harvested rapidly by washing media out once with PBS, scraping cells off plates with a cell scraper and resuspending in cell fix buffer (50mM HEPES, 1mM EDTA, 0.5mM EGTA, and 100mM NaCl), and formaldehyde-based fixing for subsequent ChIP analyses.

Immunoblot analyses

BAF complex subunits modified with Frb-V5 tags were tested for expression and complex integration using standard nuclear protein extract purification and subsequent anti-BRG1 immunoprecipitation from 150ug of nuclear extract input (anti-BRG1 (SCBT G7 clone; sc-17796)). Immunoblot analyses were performed using the antibodies indicated: BAF47 (SCBT Clone A-5; sc-166165), BAF57 (Bethyl A300-810A), SS18 (SCBT Clone H80; sc-28698), V5 epitope tag antibody (Invitrogen; R960-25).

Chromatin Immunoprecipitation (ChIP)

Briefly, for rapid time course assays, adherent CiA MEF cells were washed once in PBS, scraped off plates into fix buffer (50mM HEPES, 1mM EDTA, 0.5mM EGTA, and 100mM NaCl), resuspended, and immediately formaldehyde fixed (for 10 minutes at room temperature). After quenching cross-linking using 0.125M (final) glycine, cells ($7-10 \times 10^6$) were washed and sonicated for 13.5 minutes using a Covaris E220 Sonicator (Covaris, Inc., Woburn, MA). Chromatin input was reverse crosslinked, evaluated for shearing efficiency, and 100–150 ug of chromatin stock was used per immunoprecipitation reaction. Antibodies (3ug/ChIP reaction) used for ChIP (listed in Supplemental Table 1) were incubated with chromatin stock and Protein G Dynabeads (Cat# 1004D) overnight at 4 degrees C. Following washing, immunoprecipitated material was eluted and subjected to reverse crosslinking. Finally, DNA precipitation was performed using phenol/chloroform extraction and ChIP DNA was reconstituted in 50ul TE for qPCR reactions. Primers used in ChIP assays are listed in Supplemental Table 2.

ChIP Analysis and Statistical Calculations

CiA knock-in locus-specific primers were generated and are reflected in Table Y with plus (+) and minus (-) direction distances calculated from the middle of the ZFHD1 recruitment

domain as well as minus (+/-) distances calculated from the *Oct4* transcription start site (TSS). Briefly, enrichment (bound over input) values were normalized to values with no rapamycin treatment. Standard deviations were calculated over n=3 repeat experiments for each primer set. Student's two samples unpaired t-test was performed to determine statistical significance.

Tn5 transposase Chromatin Accessibility Assays (ATAC-qPCR)

Following various recruitment conditions, 5×10^4 CiA Oct4 MEF cells were harvested, washed once in PBS, once in RSB buffer (10mM Tris-HCl, pH 7.4, 10mM NaCl, 3mM MgCl₂), and centrifuged at $500 \times g$ for 5 minutes at 4 degrees C. Cells were then lysed in lysis buffer (500ul RSB buffer + 5ul 10% NP-40) for 5 minutes on ice, spun at $500 \times g$ for 5 minutes, resuspended in Tagment DNA/Enzyme Buffer Mix (Illumina Nextera Sample Preparation Kit, Cat. # FC-121-1030), and incubated for 30 minutes at 37 degrees C. Following Tn5 transposase enzyme reaction, DNA was purified using Quiagen MinElute PCR Purification Kit (Cat # 28004). Transposed DNA fragments were amplified via qPCR to the appropriate number of cycles and library was purified using a Quiagen PCR Cleanup Kit eluted in 20ul of elution buffer (10mM Tris Buffer, pH 8.0). CiA locus-specific qPCR was performed using primers in Supplemental Table 2.

Supplementary Material

Refer to Web version on PubMed Central for supplementary material.

Acknowledgments

We are grateful to N. Hathaway, O. Bell, L. Chen, and J. Ronan, for insightful comments and technical assistance. We thank M. Alhamadsheh for synthesis of FK1012. We also thank J. Buenrostro and B. Wu (Greenleaf Lab, Stanford University) for helpful advice and technical assistance with accessibility studies and Victoria Petkova of the BIDMC Molecular Medicine Core Facility. C.K. was supported by the NIH Director's New Innovator Award DP2 (IDP2 OD019696-01), the American Cancer Society Scholar Award (RSG-14-051-01-DMC) the Pew Scholar Award, the A.P. Giannini Foundation, the Alex's Lemonade Stand Foundation (ALSF) Young Investigator Award, and the NIH SARC Sarcoma SPORE Career Development and SPORE Project (5U54 CA168512-04) Awards. G.R.C is supported by NIH grants (CA163915, NS046789), CIRM RB4-05886, SFARI and the Howard Hughes Medical Institute.

REFERENCES

1. Kennison JA, Tamkun JW. Trans-regulation of homeotic genes in *Drosophila*. *New Biol.* 1992; 4:91–96. [PubMed: 1348185]
2. Simon JA, Kingston RE. Occupying chromatin: Polycomb mechanisms for getting to genomic targets, stopping transcriptional traffic, and staying put. *Mol Cell.* 2013; 49:808–824. [PubMed: 23473600]
3. Morgan MA, Shilatifard A. Chromatin signatures of cancer. *Genes Dev.* 2015; 29:238–249. [PubMed: 25644600]
4. Piunti A, Shilatifard A. Epigenetic balance of gene expression by Polycomb and COMPASS families. *Science.* 2016; 352:aad9780. [PubMed: 27257261]
5. Margueron R, Reinberg D. The Polycomb complex PRC2 and its mark in life. *Nature.* 2011; 469:343–349. [PubMed: 21248841]
6. Kadoch C, et al. Proteomic and bioinformatic analysis of mammalian SWI/SNF complexes identifies extensive roles in human malignancy. *Nat Genet.* 2013; 45:592–601. [PubMed: 23644491]

7. Shain AH, Pollack JR. The spectrum of SWI/SNF mutations, ubiquitous in human cancers. *PLoS One*. 2013; 8:e55119. [PubMed: 23355908]
8. Kosho T, Okamoto N. Genotype-phenotype correlation of Coffin-Siris syndrome caused by mutations in SMARCB1, SMARCA4, SMARCE1, and ARID1A. *Am J Med Genet C Semin Med Genet*. 2014; 166C:262–275. [PubMed: 25168959]
9. Santen GW, et al. Mutations in SWI/SNF chromatin remodeling complex gene ARID1B cause Coffin-Siris syndrome. *Nat Genet*. 2012; 44:379–380. [PubMed: 22426309]
10. Tsurusaki Y, et al. Mutations affecting components of the SWI/SNF complex cause Coffin-Siris syndrome. *Nat Genet*. 2012
11. Developmentalstudgroup. Large-scale discovery of novel genetic causes of developmental disorders. *Nature*. 2014
12. Ho L, et al. esBAF facilitates pluripotency by conditioning the genome for LIF/STAT3 signalling and by regulating polycomb function. *Nat Cell Biol*. 2011; 13:903–913. [PubMed: 21785422]
13. Tamkun JW, et al. brahma: a regulator of Drosophila homeotic genes structurally related to the yeast transcriptional activator SNF2/SWI2. *Cell*. 1992; 68:561–572. [PubMed: 1346755]
14. Tkachuk DC, Kohler S, Cleary ML. Involvement of a homolog of Drosophila trithorax by 11q23 chromosomal translocations in acute leukemias. *Cell*. 1992; 71:691–700. [PubMed: 1423624]
15. Kim KH, Roberts CW. Targeting EZH2 in cancer. *Nat Med*. 2016; 22:128–134. [PubMed: 26845405]
16. Varambally S, et al. The polycomb group protein EZH2 is involved in progression of prostate cancer. *Nature*. 2002; 419:624–629. [PubMed: 12374981]
17. Lee W, et al. PRC2 is recurrently inactivated through EED or SUZ12 loss in malignant peripheral nerve sheath tumors. *Nat Genet*. 2014; 46:1227–1232. [PubMed: 25240281]
18. Wu JI, Lessard J, Crabtree GR. Understanding the words of chromatin regulation. *Cell*. 2009; 136:200–206. [PubMed: 19167321]
19. Wu JI, et al. Regulation of dendritic development by neuron-specific chromatin remodeling complexes. *Neuron*. 2007; 56:94–108. [PubMed: 17920018]
20. Versteeg I, et al. Truncating mutations of hSNF5/INI1 in aggressive paediatric cancer. *Nature*. 1998; 394:203–206. [PubMed: 9671307]
21. Wilson BG, et al. Epigenetic antagonism between polycomb and SWI/SNF complexes during oncogenic transformation. *Cancer Cell*. 2010; 18:316–328. [PubMed: 20951942]
22. Kia SK, Gorski MM, Giannakopoulos S, Verrijzer CP. SWI/SNF mediates polycomb eviction and epigenetic reprogramming of the INK4b-ARF-INK4a locus. *Mol Cell Biol*. 2008; 28:3457–3464. [PubMed: 18332116]
23. Kadoch C, Crabtree GR. Reversible disruption of mSWI/SNF (BAF) complexes by the SS18-SSX oncogenic fusion in synovial sarcoma. *Cell*. 2013; 153:71–85. [PubMed: 23540691]
24. Li G, et al. Jarid2 and PRC2, partners in regulating gene expression. *Genes Dev*. 2010; 24:368–380. [PubMed: 20123894]
25. van der Stoop P, et al. Ubiquitin E3 ligase Ring1b/Rnf2 of polycomb repressive complex 1 contributes to stable maintenance of mouse embryonic stem cells. *PLoS One*. 2008; 3:e2235. [PubMed: 18493325]
26. Feldman N, et al. G9a-mediated irreversible epigenetic inactivation of Oct-3/4 during early embryogenesis. *Nat Cell Biol*. 2006; 8:188–194. [PubMed: 16415856]
27. Ho L, et al. An embryonic stem cell chromatin remodeling complex, esBAF, is an essential component of the core pluripotency transcriptional network. *Proc Natl Acad Sci U S A*. 2009; 106:5187–5191. [PubMed: 19279218]
28. Ho L, et al. An embryonic stem cell chromatin remodeling complex, esBAF, is essential for embryonic stem cell self-renewal and pluripotency. *Proc Natl Acad Sci U S A*. 2009; 106:5181–5186. [PubMed: 19279220]
29. Young RA. Control of the embryonic stem cell state. *Cell*. 2011; 144:940–954. [PubMed: 21414485]
30. Hathaway NA, et al. Dynamics and memory of heterochromatin in living cells. *Cell*. 2012; 149:1447–1460. [PubMed: 22704655]

31. Takahashi K, Yamanaka S. Induction of pluripotent stem cells from mouse embryonic and adult fibroblast cultures by defined factors. *Cell*. 2006; 126:663–676. [PubMed: 16904174]
32. Crabtree GR, Olson EN. NFAT signaling: choreographing the social lives of cells. *Cell*. 2002; 109(Suppl):S67–S79. [PubMed: 11983154]
33. Crabtree GR, Schreiber SL. Three-part inventions: intracellular signaling and induced proximity. *Trends Biochem Sci*. 1996; 21:418–422. [PubMed: 8987395]
34. Spencer DM, Wandless TJ, Schreiber SL, Crabtree GR. Controlling signal transduction with synthetic ligands. *Science*. 1993; 262:1019–1024. [PubMed: 7694365]
35. De Bruijn D. Targeted disruption of the synovial sarcoma-associated SS18 gene causes early embryonic lethality and affects PPARBP expression. *Human Molecular Genetics*. 2006; 15:2936–2944. [PubMed: 16926188]
36. Banaszynski LA, Liu CW, Wandless TJ. Characterization of the FKBP:rapamycin:FRB ternary complex. *J Am Chem Soc*. 2005; 127:4715–4721. [PubMed: 15796538]
37. Schuettengruber B, Chourrout D, Vervoort M, Leblanc B, Cavalli G. Genome regulation by polycomb and trithorax proteins. *Cell*. 2007; 128:735–745. [PubMed: 17320510]
38. Blackledge NP, et al. Variant PRC1 complex-dependent H2A ubiquitylation drives PRC2 recruitment and polycomb domain formation. *Cell*. 2014; 157:1445–1459. [PubMed: 24856970]
39. Kadoch C, Crabtree GR. Mammalian SWI/SNF chromatin remodeling complexes and cancer: Mechanistic insights gained from human genomics. *Sci Adv*. 2015; 1:e1500447. [PubMed: 26601204]
40. Yen K, Vinayachandran V, Batta K, Koerber RT, Pugh BF. Genome-wide nucleosome specificity and directionality of chromatin remodelers. *Cell*. 2012; 149:1461–1473. [PubMed: 22726434]
41. Lorch Y, Zhang M, Kornberg RD. Histone octamer transfer by a chromatin-remodeling complex. *Cell*. 1999; 96:389–392. [PubMed: 10025404]
42. Mendenhall EM, et al. GC-rich sequence elements recruit PRC2 in mammalian ES cells. *PLoS Genet*. 2010; 6:e1001244. [PubMed: 21170310]
43. Deal RB, Henikoff JG, Henikoff S. Genome-wide kinetics of nucleosome turnover determined by metabolic labeling of histones. *Science*. 2010; 328:1161–1164. [PubMed: 20508129]
44. Buenrostro JD, Giresi PG, Zaba LC, Chang HY, Greenleaf WJ. Transposition of native chromatin for fast and sensitive epigenomic profiling of open chromatin, DNA-binding proteins and nucleosome position. *Nat Methods*. 2013; 10:1213–1218. [PubMed: 24097267]
45. Jadhav U, et al. Acquired Tissue-Specific Promoter Bivalency Is a Basis for PRC2 Necessity in Adult Cells. *Cell*. 2016; 165:1389–1400. [PubMed: 27212235]
46. Schnitzler G, Sif S, Kingston RE. Human SWI/SNF interconverts a nucleosome between its base state and a stable remodeled state. *Cell*. 1998; 94:17–27. [PubMed: 9674423]
47. Ronan JL, Wu W, Crabtree GR. From neural development to cognition: unexpected roles for chromatin. *Nat Rev Genet*. 2013; 14:347–359. [PubMed: 23568486]
48. Khavari PA, Peterson CL, Tamkun JW, Mendel DB, Crabtree GR. BRG1 contains a conserved domain of the SWI2/SNF2 family necessary for normal mitotic growth and transcription. *Nature*. 1993; 366:170–174. [PubMed: 8232556]
49. Narayanan R, et al. Loss of BAF (mSWI/SNF) Complexes Causes Global Transcriptional and Chromatin State Changes in Forebrain Development. *Cell Rep*. 2015; 13:1842–1854. [PubMed: 26655900]
50. Yoo AS, Staahl BT, Chen L, Crabtree GR. MicroRNA-mediated switching of chromatin-remodelling complexes in neural development. *Nature*. 2009; 460:642–646. [PubMed: 19561591]
51. Yoo AS, et al. MicroRNA-mediated conversion of human fibroblasts to neurons. *Nature*. 2011; 476:228–231. [PubMed: 21753754]
52. Victor MB, et al. Generation of human striatal neurons by microRNA-dependent direct conversion of fibroblasts. *Neuron*. 2014; 84:311–323. [PubMed: 25374357]
53. Singhal N, et al. Chromatin-Remodeling Components of the BAF Complex Facilitate Reprogramming. *Cell*. 141:943–955.
54. Lickert H, et al. Baf60c is essential for function of BAF chromatin remodelling complexes in heart development. *Nature*. 2004; 432:107–112. [PubMed: 15525990]

55. Tea JS, Luo L. The chromatin remodeling factor Bap55 functions through the TIP60 complex to regulate olfactory projection neuron dendrite targeting. *Neural Dev.* 2011; 6:5. [PubMed: 21284845]
56. Weinberg P, Flames N, Sawa H, Garriga G, Hobert O. The SWI/SNF chromatin remodeling complex selectively affects multiple aspects of serotonergic neuron differentiation. *Genetics.* 2013; 194:189–198. [PubMed: 23457234]
57. Dawson MA, Kouzarides T. Cancer epigenetics: from mechanism to therapy. *Cell.* 2012; 150:12–27. [PubMed: 22770212]

Author Manuscript

Author Manuscript

Author Manuscript

Author Manuscript

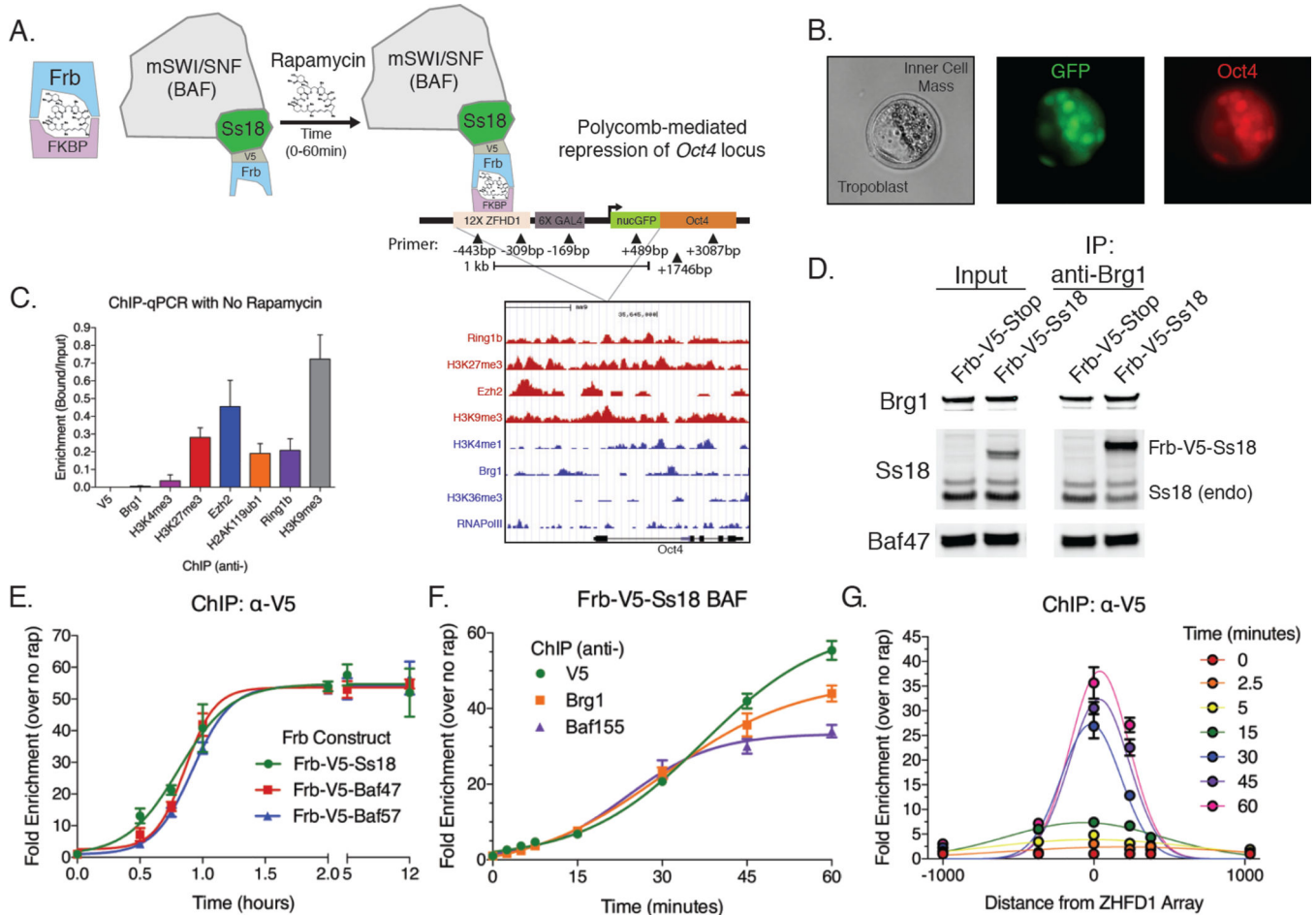


Figure 1. Design and development of a rapidly-inducible system to recruit BAF complexes to heterochromatin in vivo

(a) Recruitment schematic for Frb-tagged BAF complexes by rapamycin in MEFs to the Oct4 (*Pou5f1*) locus. Rapamycin (FK506) dimerizes Frb and FKBP. Primer distances are distances from Oct4 TSS. (b) Mouse embryos with recruitment system and CiA-modified Oct4 allele (GFP) exhibit normal embryonic development and similar Oct4 expression from the inserted allele and the wild-type allele in blastocysts. (c) ChIP-qPCR and ChIP-seq for repressive and activating marks indicates large-scale repression of the Oct4 locus. (Error bars = Mean \pm SD for n=10 experiments). (d) Total nuclear input and anti-Brg1 immunoprecipitation shows Frb-V5-Ss18 properly assembles into BAF complexes. (e) BAF complex recruitment (ChIP-qPCR fold enrichment over no rapamycin treatment at the ZFHD1 site (-443bp)) can be achieved using several different Frb-tagged BAF subunits. BAF complex recruitment reaches saturation by 1.5 hours. (f) Anti-Brg1, anti-Baf155 ChIP-qPCR demonstrates that Frb-V5-Ss18 recruits the complete BAF complex to the ZFHD1 recruitment site (-443bp). (g) Landscape plot of anti-V5 ChIP-qPCR data demonstrates BAF complex regional occupancy over a t= 0–60min time course. BAF domain spread is 920 ± 305 bp from the ZFHD recruitment site (95% confidence interval). Error bars = Mean \pm SD for n=3 experiments in (e-g).

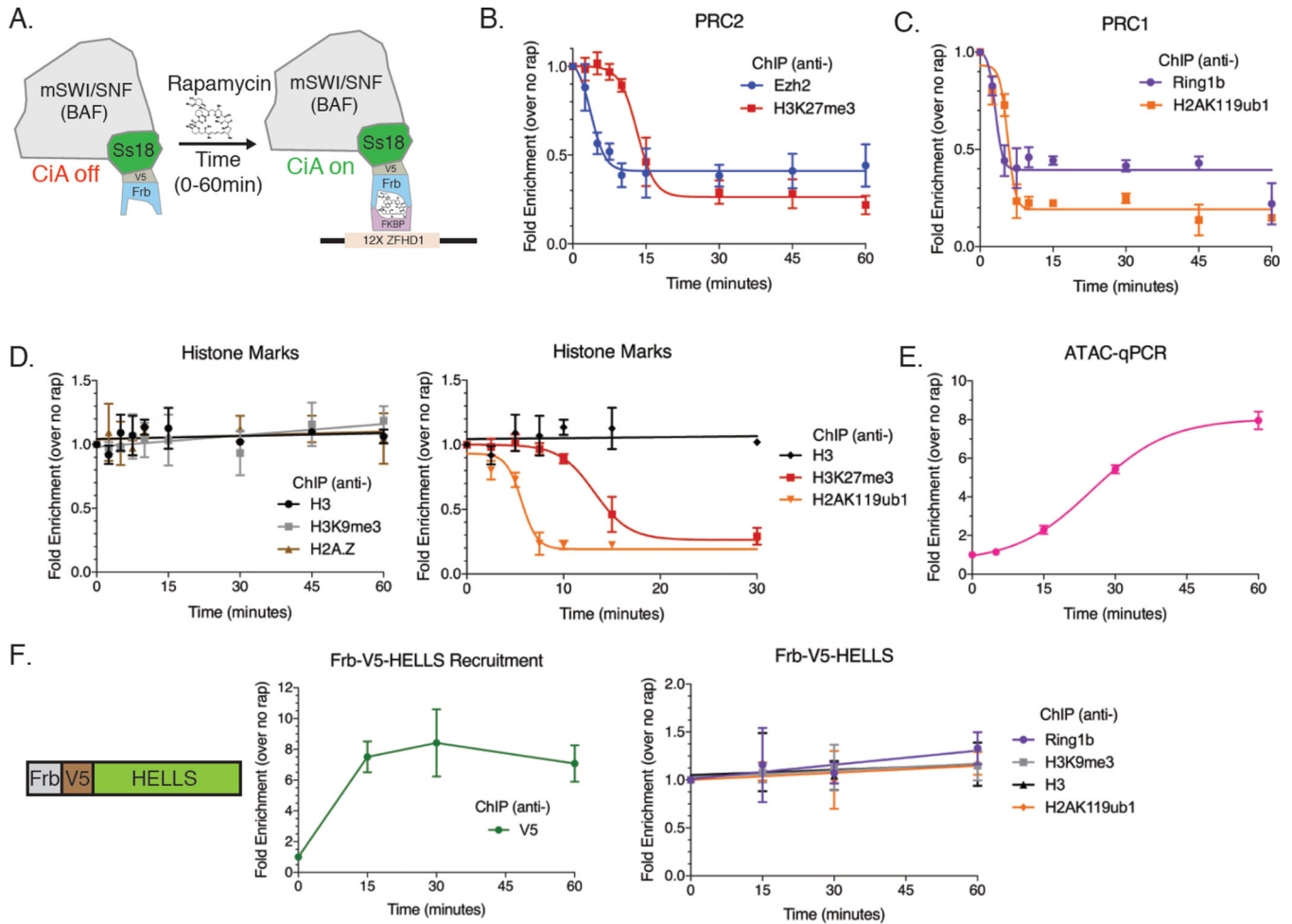


Figure 2. BAF complexes displace PcG repression upon recruitment

(a) Schematic for rapamycin-induced recruitment of Frb-V5-Ss18 BAF complexes. (b-c) BAF complex recruitment results in (b) Ezh2 displacement within 10 min followed by H3K27me3 removal within 20 min, and (c) Ring1b displacement within 5 min followed by H2AK119ub1 removal within 7.5min (at -443bp ZFHD1 site). (d) Total histone (H3) occupancy and non-PcG histone marks (H3K9me3, H2A.Z) are unaffected by BAF complex recruitment (left). Comparison of H3 levels to PcG marks shows removal of PRC1 repression followed by removal of PRC2 repression, with H3 unchanged (right). (e) ATAC-qPCR at ZFHD recruitment site (-443bp) shows increase in DNA accessibility upon BAF complex recruitment. (f) The HELLs (LSH) chromatin remodeler shows rapid recruitment via rapamycin-recruitment system (left), however PRC1 and PRC1-placed repressive marks are not displaced (right), nor are H3K9me3 or total H3. All ChIP-qPCR measurements are at the -443bp ZFHD1 site. Error bars = Mean \pm SD for n=3 experiments except (c) for n=2 experiments.

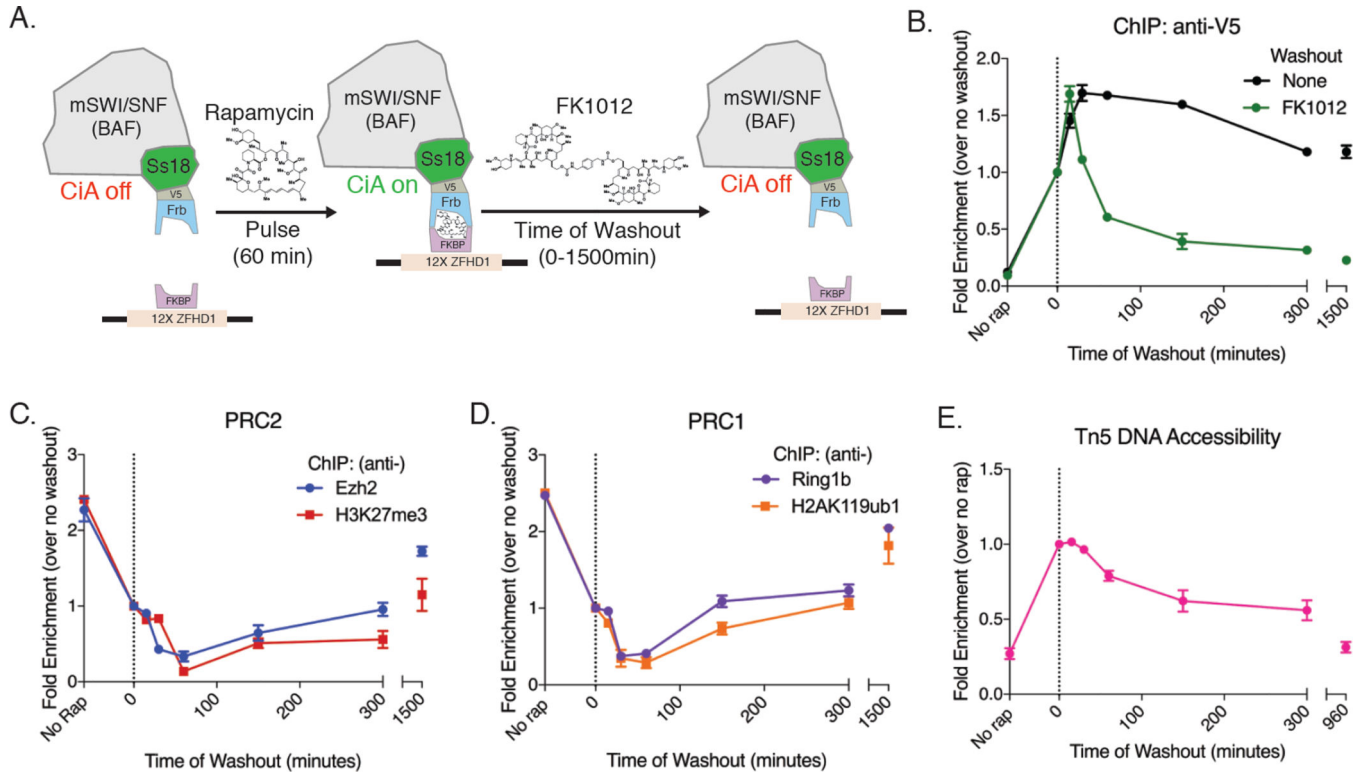


Figure 3. Rapid removal of BAF complexes by competitive inhibition of rapamycin triggers reformation of repressed heterochromatin

(a) Schematic for FK1012-driven washout of rapamycin-tethered BAF complexes. (b) Comparison of BAF occupancy upon FK1012-driven washout to no washout (media exchange). (c-d) FK1012 washout triggers show reformation of heterochromatin, with (c) PRC2 and (d) PRC1 repression beginning to reform within hours. (e) ATAC-qPCR at recruitment shows accessibility is lost upon FK1012 washout and reformation of heterochromatin. All ChIP-qPCR measurements are at the -443bp ZFH1 site. Error bars = Mean \pm SD for n=3 experiments.

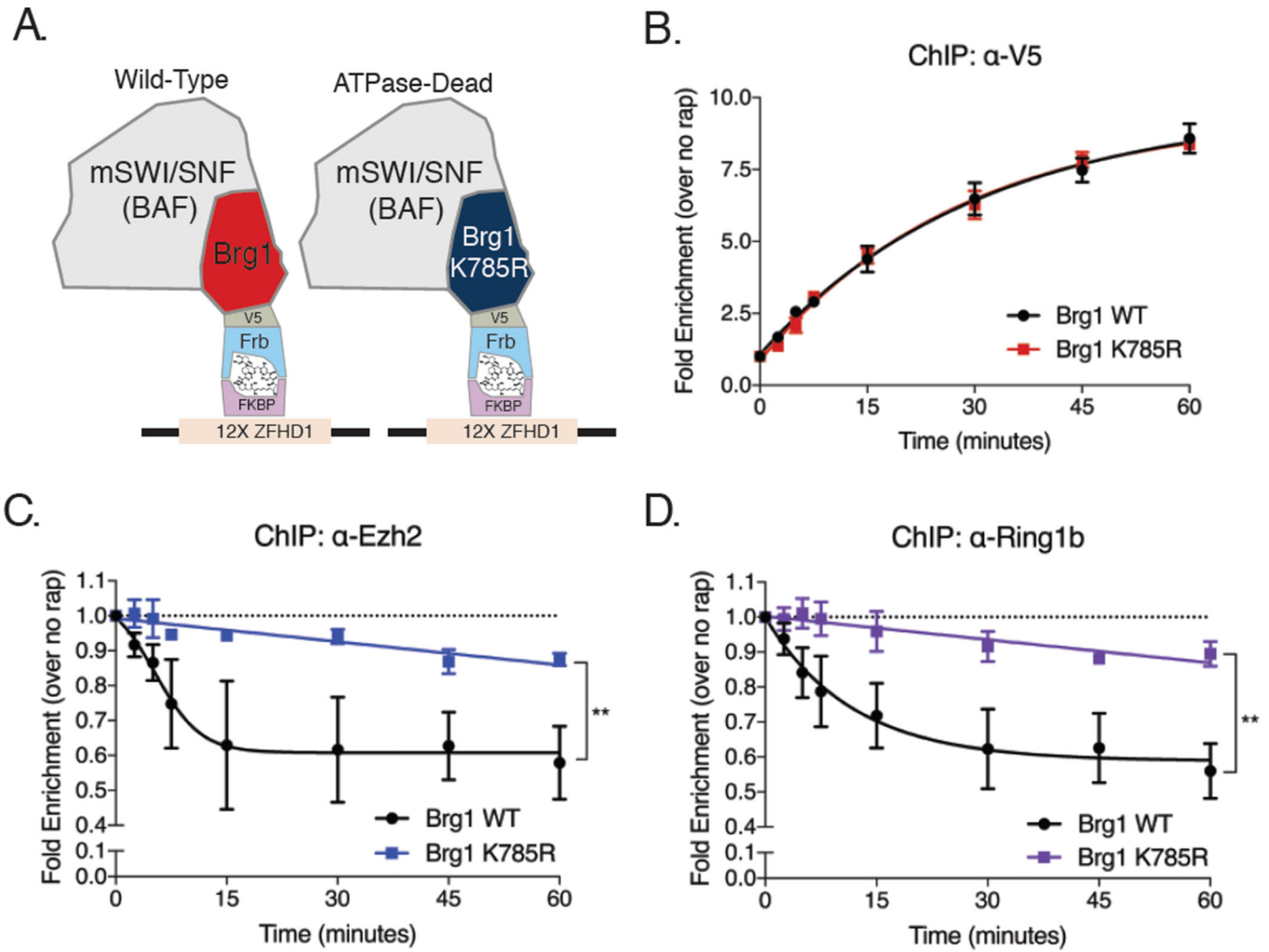


Figure 4. BAF complex-mediated eviction of Polycomb is ATP-dependent
(a) Brg1-V5-Frb system for rapidly recruiting BAF complexes containing wild-type Brg1 or ATPase-dead Brg1 (K785R mutant). **(b)** BAF complex recruitment to the ZHFD1 recruitment site with wild-type and ATPase-dead Brg1 is comparable. **(c-d)** Eviction of PcG proteins is dependent on ATPase function, with **(c)** Ezh2 and **(d)** Ring1b eviction reduced with ATPase-dead Brg1 as compared to wild-type Brg1. All ChIP-qPCR measurements are at the -443bp ZFHD1 site. Error bars = Mean ± SD for n=3 experiments. (** p-value < 0.01).

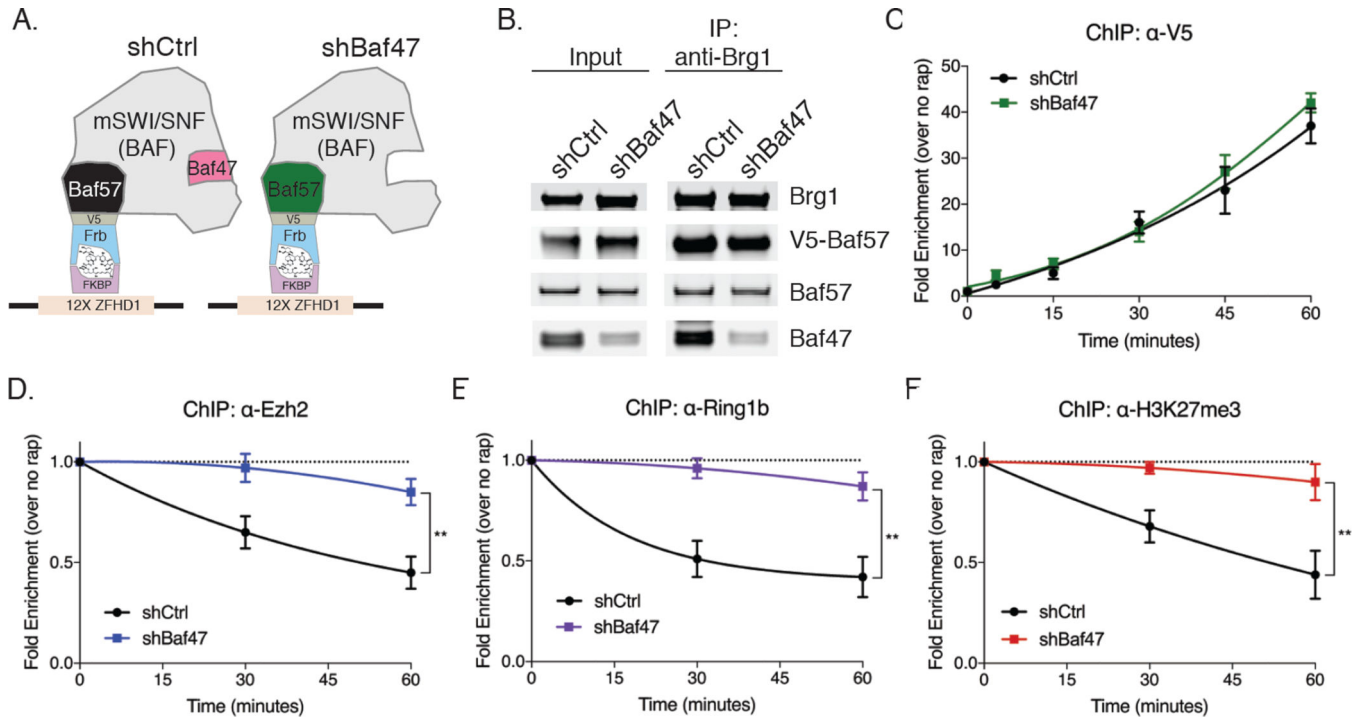


Figure 5. Baf47-deficient (MRT-like) BAF complexes fail to evict PcG repression
(a) Frb-V5-Baf57 system for rapidly recruiting BAF complexes lacking Baf47. **(b)** Total nuclear input and anti-Brg1 in BAF complexes. **(c)** BAF complexes in shCtrl and shBaf47 cells display comparable recruitment at ZHFHD1 recruitment locus. **(d-f)** MRT-like BAF complexes (lacking Baf47) fail to evict PcG proteins at ZHFHD1 recruitment site, with **(d)** Ezh2, **(e)** Ring1b, and **(f)** H3K27me3 evicted by wild-type BAF but not by MRT-like BAF. All ChIP-qPCR measurements are at the -443bp ZFHD1 site. Error bars = Mean \pm SD for n=3 experiments. (** p-value < 0.01)

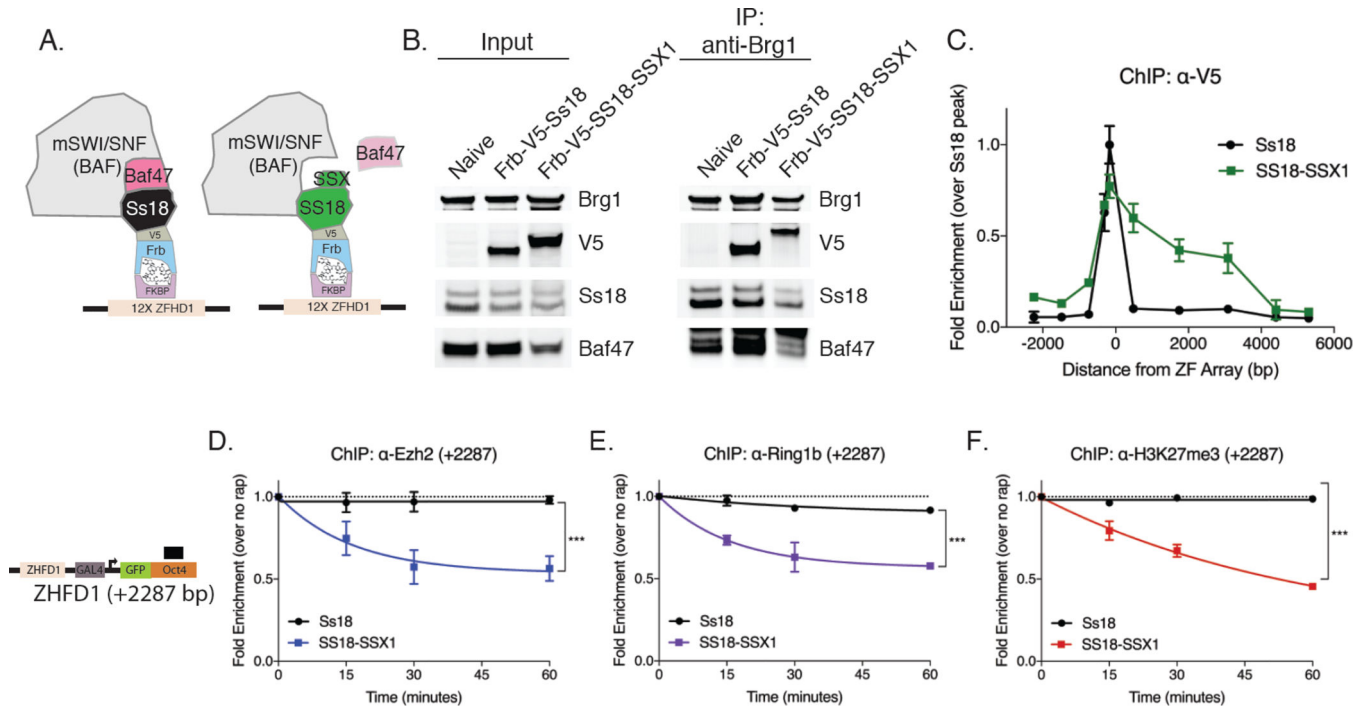


Figure 6. SS18-SSX-containing (SS-like) BAF complexes exhibit enhanced occupancy and Polycomb eviction

(a) Schematic of Frb-V5-Ss18 (WT) versus Frb-V5-SS18-SSX1 fusion (SS-like) for comparison of wild-type versus oncogenic BAF complexes. (b) Nuclear extract input and anti-V5 immunoprecipitation in cells with tagged Ss18 or SS18-SSX1. (c) Landscape plot reflecting enhanced occupancy of SS18-SSX1-containing BAF complexes as compared to wild-type (Ss18) around ZHFD1 recruitment site, into the Oct4 gene body. (d-f) SS-like BAF complexes exhibit enhanced downstream (+2287bp) PcG eviction over the Oct4 gene body of Ezh2 (d), Ring1b (e), and H3K27me3 (f). All ChIP-qPCR measurements in (d-f) are at the +1716bp ZFHD1 site. Error bars = Mean \pm SD for n=3 experiments. (***) p-value < 0.001).

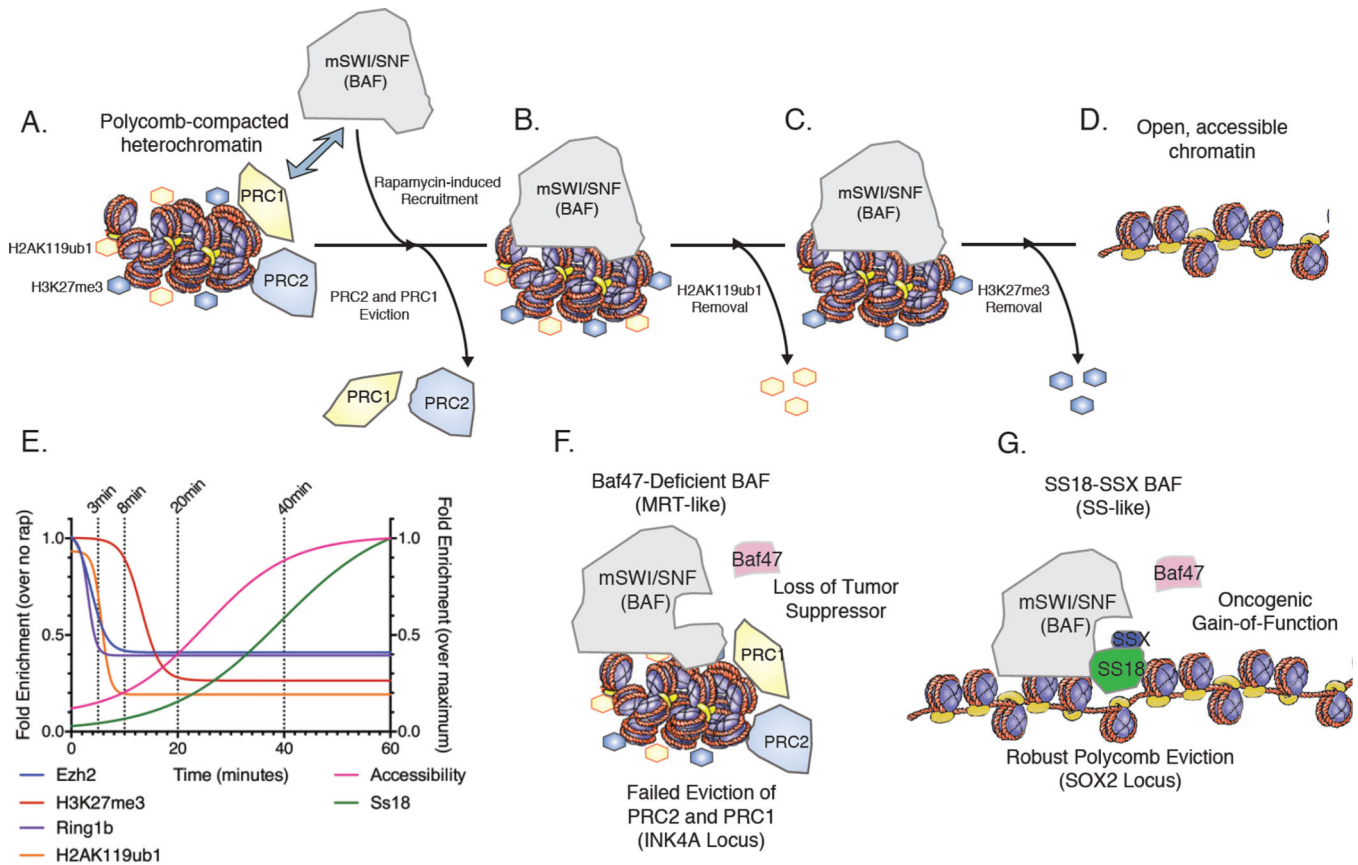


Figure 7. Model for rapid BAF-PcG opposition in normal and oncogenic settings

(a) BAF complex recruitment via Frb-V5-SS18 system begins to displace PRC2 (Ezh2) and PRC1 (Ring1b) by 3 min after rapamycin treatment. (b) H2AK119ub1 marks are rapidly removed from histones, with removal complete after 8 min of rapamycin treatment. (c) H3K27me3 begins removal upon completion of H2AK119ub1 removal, with removal complete by 20 min. (d) DNA accessibility accelerates upon removal of H3K27me3, with 90% maximum accessibility within 40 min. (e) Time-dependent representation of PcG eviction and accessibility gain with BAF recruitment. (f) Tumor suppressor Baf47-deficient BAF complexes fail to evict PRC2 and PRC1, resulting in heterochromatin and repression of key tumor suppressors, such as INK4A. (g) Oncogenic, gain-of-function SS18-SSX BAF complexes exhibit enhanced occupancy and robust eviction of PRC2 and PRC1, resulting in open chromatin and expression of oncogene SOX2.